Lepidocrocite to maghemite to hematite:

A way to have magnetic and hematitic Martian soil

RICHARD V. MORRIS[1*], D. C. GOLDEN[2], TAD D. SHELFER[3], AND H. V. LAUER, Jr[4].

[1]Mail Code SN3, NASA Johnson Space Center, Houston, Texas 77058, USA

[2]Dual Inc., Houston, Texas, 77058, USA

[3]Viking Science & Technology, Inc., 16821 Buccaneer Ln, Houston, Texas 77058, USA

[4]Lockheed Martin Space Mission Systems & Services, Houston, Texas 77058, USA

*Correspondence author's e-mail address: rvmorris@ems.jsc.nasa.gov

(Submitted to *Meteoritics and Planetary Science*, October, 1997)

Abstract - We examined decomposition products of lepidocrocite, which were produced by heating the phase in air at temperatures up to 525°C for 3 and 300 hr, by XRD, TEM, magnetic methods, and reflectance spectroscopy (visible and near-IR). Single-crystal lepidocrocite particles dehydroxilated to polycrystalline particles of disordered maghemite which subsequently transformed to polycrystalline particles of hematite. Essentially pure maghemite was obtained at 265 and 223°C for the 3 and 300 hr heating experiments, respectively. Its saturation magnetization (J_s) and mass specific susceptibility are ~50 Am^2/kg and ~40 $\mu m^3/kg$, respectively. Because hematite is spectrally dominant, spectrally-hematitic samples (i.e., characterized by a minimum near 860 nm and a maximum near 750 nm) could also be strongly magnetic (J_s up to ~30 Am^2/kg) from the masked maghemite component. TEM analyses showed that individual particles are polycrystalline with respect to both maghemite and hematite. The spectrally-hematitic and magnetic Mh+Hm particles can satisfy the spectral and magnetic constraints for Martian surface materials over a wide range of values of Mh/(Mh+Hm) and as either pure oxide powders or (within limits) as components of multiphase particles. These experiments are consistent with lepidocrocite as the precursor of Mh+Hm assemblages on Mars, but other phases (e.g., magnetite) that decompose to Mh and Hm are also possible precursors. Simulations done with a copy of the Mars Pathfinder Magnet Array showed that spectrally hematitic Mh+Hm powders having J_s equal to 20.6 Am^2/kg adhered to all five magnets.

INTRODUCTION

The magnetic mineralogy of Martian soil has been investigated by both the Viking (1976) and Pathfinder (1997) missions to the planet. The results of the Viking magnetic properties experiment indicate the presence of 1-7 wt % of a highly magnetic phase that is most probably present as a minor component of composite particles rather than as discrete magnetic grains (Hargraves *et al.*, 1977, 1979; Moskowitz and

Hargraves, 1982; Posey-Dowty *et al.*, 1986). The preferred interpretation of Hargraves and coworkers is that the strongly magnetic phase is the ferric oxide maghemite (γ-Fe_2O_3). Moskowitz and Hargraves (1982) note that if either magnetite or maghemite is the strongly magnetic phase, the saturation magnetization for Martial soil approaches 1-7 Am^2/kg. Using the lessons learned from the Viking results and hardware design, more sophisticated magnetic properties experiments were designed and built for the Pathfinder mission (Smith *et al.*, 1997). They have the capability to better define the saturation magnetization and mode of occurrence of magnetic phases on Mars.

If we accept that maghemite is present in Martian soil as a working hypothesis, how did it form? It is well known (e.g., Cornell and Schwertmann, 1996, and references therein) that maghemite is the immediate dehydroxylation product of lepidocrocite (γ-FeOOH), and Hargraves *et al.* (1977) suggested the phase as a possible precursor for maghemite on Mars. Posey-Dowty (1986) and Banin *et al.* (1993) developed this idea further through experimental investigations directed at showing that lepidocrocite, and not goethite (α-FeOOH), might be the favored weathering product on Mars. Goethite is the FeOOH polymorph usually formed in terrestrial weathering environments (e.g., Cornell and Schwertmann, 1996). If this line of reasoning is correct, we might expect to observe evidence for both lepidocrocite and maghemite in Martian spectral data. Is this the case?

Spectral data at visible and near-IR wavelengths for typical Martian bright regions are characterized by a ferric absorption edge extending from ~400 to 750 nm with superimposed weak features near 600 nm (a shoulder), 750 nm (a reflectivity maximum), and 860 nm (a reflectivity minimum) (e.g., Mustard and Bell, 1994). The spectrum is attributed to nanophase ferric oxide particles plus lesser amounts (<5%) of red (i.e., well-crystalline and pigmentary) hematite (e.g., Morris *et al.*, 1997). Nanophase ferric oxide particles are primarily responsible for the absorption edge, and the weak features are manifestations of hematite. Morris and Golden (1997) showed that hematitic Martian spectral data permit the presence of some goethite, because the characteristic goethite spectral features (e.g., the

minimum near 900 nm) are overwhelmed by those for hematite and not observed. Presumably, similar results apply to other ferric bearing phases, but this has not been demonstrated. In addition to hematitic regions, there are other, areally more restricted Martian bright regions that have weak minima near 900 nm (Murchie *et al.*, 1993). This position is consistent with many ferric-bearing mineralogies, including goethite, jarosite, nontronite, and maghemite. Thus, the spectral evidence is that there are at least two crystalline and ferric-bearing mineralogies in the optical surface on Mars. One of them is most likely hematite, and the mineralogy of the other is equivocal but could be maghemite.

In this paper, we investigate the idea, originally proposed by Hargraves *et al.* (1979) that the magnetic and spectral properties of Martian bright regions can be accommodated by the presence of both maghemite and hematite. To do this, we studied the magnetic and spectral properties of samples of lepidocrocite heated at various times and temperatures to produce samples having variable proportions of lepidocrocite, maghemite, and hematite. In this way, we start with a phase (lepidocrocite) which might form as a product of weathering on Mars (Posey-Dowty *et al.*, 1986; Banin *et al.*, 1993) and whose thermal transformation products (maghemite and hematite) could account for the magnetic and certain spectral properties of the Martian surface. A magnet array equivalent to those on the Mars Pathfinder lander was used to obtain magnetic properties that are directly comparable to those obtained on the Martian surface.

SAMPLES AND METHODS

The lepidocrocite used for the heating experiments is LPS2 described by Morris *et al.* [1985]. It is a synthetic, well-crystalline lepidocrocite. The heating experiments were done in air at various temperatures between 55 and 525°C. The period of heating at temperature was generally ~3 hr, although some samples were heated for 300 hr. The samples included in this study are listed in Table 1. Sample identification (e.g., LPS2-3-256) includes the heating time (3 hr) and temperature (265°C).

Thermogravimetric data and values of the saturation magnetization (J_s) for samples heated for 3 hr are reported by Morris and Lauer (1981). X-ray diffraction data were obtained using a Scintag 2000XDS X-ray diffractometer using CuKα radiation. A JEOL 2000Fx transmission electron microscope (TEM) operated at 200 kV was employed for TEM imaging and selected area electron diffraction (hereafter referred to as electron diffraction). Saturation magnetizations and mass specific susceptibilities (X_m) were obtained at room temperature on a PAR Model 155 Vibrating Sample Magnetometer and a Bartington Model MS2 magnetic susceptibility meter, respectively. Diffuse reflectance spectra (350-2100 nm) were obtained on a Cary-14 spectrometer configured with a 23-cm diameter integrating sphere. Positions of spectral features (maxima and minima) were determined from the zero values of first derivatives of reflectivity spectra.

A magnet array (MA), which is identical to the ones flown on Mars Pathfinder (Smith *et al.*, 1997) except for the surface coating, was used to determine Pathfinder-style magnetic properties for some of our transformation products. Basically, it consists of five permanent magnets having different attractive forces. The MA was made at the Oersted Laboratory, Niels Bohr Institute for Astronomy, Physics, and Geophysics, University of Copenhagen, Denmark, and provided courtesy of Drs. Jens Martin Knudsen and Morton Bo Madsen. Particulate material was presented to the MA by placing powder in a 7.6-cm diameter sieve that has holes 90 μm in diameter. The sieve was then tapped with a metal rod while holding it ~5-10 cm above the MA. This procedure produced a "cloud" of particles below the sieve which settled toward the MA. Particles preferentially accumulated on the magnets where the attractive force was sufficiently strong. The surface of the MA makes an angle of 30° with respect to the horizontal. Results were documented photographically with a digital camera (Kodak Model DC120).

LEPIDOCROCITE TO MAGHEMITE TO HEMATITE

XRD and TEM Analyses

Representative XRD data for samples heated for 3 hr are shown in Fig. 1. The phases present are noted on the figure and compiled in Table 1. The diffraction lines whose indexes are noted on the figure ([020], [120], and [051] for lepidocrocite; [220] and [440] for maghemite; [012], [104], and [113] for hematite) are specific for one of the three phases. Thus, for the 3 hr heating experiments, lepidocrocite (Lp) is not detected after the 233°C step. Maghemite (Mh) first appears at 223°C, reaches maximum abundance at 265°C, and is just barely observed at 384°C. Hematite (Hm) is clearly present at 233°C, and is the only phase detected at 450°C and higher temperatures. The same trends are observed in the 300 hr heating experiments, except that the phase changes occur at lower temperatures. For example, maximum Mh concentrations (equivalently, no Lp remaining) occur at ~223 and 265°C for the 300 and 3 hr heating periods, respectively.

The XRD lines for Mh in sample LPS2-3-265, which has the highest proportion of Mh for the 3-hr experiments, are considerably broader than those for either Lp or Hm in samples that contain mostly those phases. These differences imply that the maghemite crystallites are too small for cation and vacancy ordering to to take place. In Fig. 2, the XRD spectra for LPS2-3-265 and LPS2-300-223, the two samples with the most Mh, are compared with a spectrum for well-crystalline maghemite MHS3, which is a synthetic product made commercially by reduction of acicular goethite to acicular magnetite and subsequent oxidation of the magnetite to maghemite (Morris *et al.*, 1985). Note the difference in the width of the XRD lines between the two samples and the presence of the tetragonal superlattice lines in MHS3 but not the maghemites derived from LPS2. These differences result from complete ordering of the vacancies on octahedral sites for MHS3 but not for the maghemites obtained from LPS2 (e.g., Cornell and Schwertmann, 1996).

As shown in TEM micrographs (Fig. 3), the lepidocrocite particles (LPS2) prior to heating were lath-shaped, elongated in the crystallographic "*c*" direction and occur as bundles. Individual laths were 1-2 μm in length and ~20 nm in width. These crystals give a sharp electron diffraction pattern (Fig. 3a) indicative of ordered single crystals. Upon heating to 223°C, the crystal morphology remains unchanged while new diffraction spots appear indicating partial transformation to maghemite (Fig. 3b). The disordered nature of the maghemite is shown by diffuse streaking spots. At 265°C the morphology is still that of the original lepidocrocite, but the diffraction pattern consists entirely of diffuse, streaky spots resulting from maghemite (Fig. 3c). In the sample heated to 323°C, the streaky maghemite spots are still present, but some hematite spots or rings resulting from polycrystalline diffraction appear (Fig. 3d). The hematite and maghemite are both poorly ordered. At 500°C, all particles have fully converted to polycrystalline, well-ordered hematite, as shown by the ring pattern formed by the large number of discrete spots (Fig. 3e). In addition, magnified images show obvious rounded edges (Fig. 3f), although overall the particles retain the shape of the lepidocrocite precursor. Changes in morphology suggest increased mobility of the atoms in the oxide phase at 500°C.

Our XRD and TEM results are consistent with literature data (as summarized by Cornell and Schwertmann, 1997) for the thermal decomposition of lepidocrocite to maghemite and maghemite to hematite. Our XRD data for nearly pure maghemites LPS2-3-265 and LPS2-300-223 (Fig. 2) are very similar to those reported by De Bakker *et al.* (1991), who used 1 hr heating periods. Because the temperatures for the Lp→Mh and Mh→Hm transitions depend on heating period (discussed below), it is not possible to correlate results with heating temperature. However, our hematites, like those of De Bakker *et al.* (1991), are well-ordered compared to their maghemite precursor.

XRD and TEM analyses are in agreement as to phases present and disordered nature of maghemite (broad diffraction lines and streaky ED spots) produced by thermal decomposition of lepidocrocite. TEM analyses provide the microscale results that (1) the acicular particle morphology of lepidocrocite is retained

throughout the transformation, (2) the initially single-crystal lepidocrocite particles transform to polycrystalline maghemite and hematite particles, and (3) individual particles are multiphase when more than one phase is present. The first two results mean that the maghemite and hematite are polycrystalline pseudomorphs after lepidocrocite. Discrete, multiphase particles (e.g., maghemite and hematite) mean that spectral and magnetic properties, which are measured for bulk samples, are derived from the properties of discrete particles and do not represent the average of a mixture of particles having different individual mineralogies.

Magnetic Properties

Values of saturation magnetization (J_s) and mass specific susceptibility (X_m) for the heated samples are compiled in Table 1 and plotted as a function of heating temperature in Fig. 4. Because neither lepidocrocite or hematite are strongly magnetic compared to maghemite (Morris *et al.*, 1985), the formation of maghemite from dehydroxylation of lepidocrocite and its subsequent rearrangement to hematite are readily observed in the magnetic data. Both transformations are kinetically controlled because the transformation temperatures depend on the period of heating. For example, dehydroxylation of lepidocrocite to maghemite occurs in the intervals ~140-190°C and ~180-230°C for the ~300 hr and ~3 hr heating periods, respectively. Gehring and Hofmeister (1994), using heating periods of 0.5 hr, report dehydroxylation in the interval 175-300°C for their bulk susceptibility data. The thermogravimetric data of Morris and Lauer (1981) for LPS2 and De Bakker *et al.* (1991) for lepidocrocite L86 show dehydroxylation (measured as weight loss) in the interval ~190-240°C (heating rate of 30°C/hr) and ~200-275°C (heating rate of 120°C/hr), respectively. Because of differences in heating method (isothermal at each temperature versus continuous) and the sensitivity of the dehydroxylation temperature to heating rate, the magnetic and thermogravimetric data for LPS2 are in good agreement.

The maximum value we observe for J_s is ~50 Am^2/Kg (Table 1). This value, which was obtained for both 3 and 300 hr heating periods, is considerably less than the value of 74 Am^2/kg measured for maghemite MHS3 (Morris *et al.*, 1985) and for the range that is usually cited in the literature for maghemites (60-80 Am^2/kg; e.g., Cornell and Schwertmann, 1996). Presumably, the lower values measured for maghemites derived from lepidocrocite result from the their low degree of vacancy ordering and small crystallite size (broad XRD lines and no tetragonal superlattice lines) compared to the high degree of vacancy ordering for MHS3 (narrow lines and tetragonal superlattice lines) as can be seen in Fig. 2. The small amounts of hematite that are present in maghemites derived from LPS2 (LPS2-3-265 and LPS2-300-223; Fig. 2) would also lower the values of J_s.

Mass specific susceptibility data reported by Gehring and Hofmeister (1994) for lepidocrocite and its maghemite dehydroxylation product range from 0.62 $\mu m^3/kg$ for unheated lepidocrocite to a maximum of 1260 $\mu m^3/kg$ for maghemite. Our value for lepidocrocite LPS2 (Table 1) is within a factor of 2 (1.1 $\mu m^3/kg$), but our value for maghemite (40 $\mu m^3/kg$) is a factor of 32 lower. The reason for such a large difference could be related to differences in particle size and/or shape (e.g., Cornell and Schwertmann, 1996). Such differences would also tend to lower J_s, but Gehring and Hofmeister (1994) did not report a J_s for their maghemite.

Comparison of magnetic and XRD data show that the former are more sensitive to small amounts of maghemite. The XRD spectrum of LPS2-3-200 does not have detectable lines from maghemite (Fig. 1), but, based on J_s data, has ~6% maghemite (using 50 Am^2/kg for J_s for "pure" maghemite from lepidocrocite).

Spectral Properties

The reflectivity spectra of samples of LPS2 heated for 3 hr are shown in Fig. 5. The spectra are organized into three groups depending on the positions of their T1 and M1 spectral features. T1 and M1

are the lowest-energy minimum and maximum, respectively, for spectral features associated with ferric-iron. In a pure ferric oxide, the T1 minimum corresponds to the position of the $^6A_1 \rightarrow {}^4T_{1g}$ ferric electronic transition, and M1 corresponds to the reflectivity maximum between the $^6A_1 \rightarrow {}^4T_{1g}$ and $^6A_1 \rightarrow {}^4T_{2g}$ ferric transitions. In mixtures of ferric oxides, T1 and M1 are the measured positions of the lowest-energy minimum and maximum envelopes (or composite bands) defined by the individual transitions which, in general, occur at different energies. The upper, middle, and lower groups of spectra in Fig. 5 are, spectrally speaking, lepidocrocite, maghemite, and hematite.

The positions of the T1 and M1 spectral features are shown as a function of heating temperature and time in Fig. 6. If this figure were considered alone, it could be interpreted as thermal dehydroxylation of lepidocrocite to hematite without passing through maghemite. In this case, the intermediate values of T1 and M1 in the transition region (~150-325°C) represent the positions of envelopes formed from lepidocrocite and hematite bands. However, we know from the XRD and magnetic data that this is not the case. The values of T1, for example, in the region 890-930 nm result from samples that are predominantly maghemite based on XRD data and have the highest values of J_s (Table 1). For comparison, the values of T1 reported by Morris *et al.* (1985) for maghemites synthesized via magnetite are ~920-940 nm. The apparently somewhat lower values of T1 for maghemites derived from lepidocrocite compared to those derived from magnetite may be related to structural order or perhaps to small amounts of hematite observed in XRD data. Maghemite is not present over a sufficiently large temperature interval for plateaus to develop in either the M1 or M2 data (Fig. 6).

APPLICATION TO MARS

As discussed in the Introduction, two types of data available for Martian surface materials are reflectivity spectra and magnetic properties. Reflectivity spectra of Martian bright regions that have spectral feature near 620, 750 and 860 nm are interpreted as having red hematite as an optically important

component whose abundance is likely <5% (Morris *et al.*, 1997). The results of the Viking magnetic properties experiment show that Martian soil is magnetic (J_s ~1-7 Am^2/kg), and the preferred interpretation of Hargraves and coworkers is that maghemite, a strongly-magnetic phase, is present as a component of composite (multiphase) soil particles (Hargraves *et al.*, 1977, 1979; Moskowitz and Hargraves, 1982; Posey-Dowty *et al.*, 1986). Although other magnetic materials have been advanced to explain the magnetic properties of the Martian surface, our purpose here is to address issues involving the simultaneous presence of both hematite and maghemite. Specifically, can hematite-maghemite assemblages satisfy both the spectral and magnetic constraints for the Martian surface? Are the constraints satisfied for a narrow or wide interval in the hematite-maghemite binary system? Is it reasonable for such assemblages to form on Mars?

Fig. 7 is a plot of J_s versus positions of the T1 and M1 spectral features for both 3 and 300 hr heating intervals. The regions that are characterized by the spectral signatures of either hematite or lepidocrocite are indicated by the stippling. The hematitic region corresponds to over three orders of magnitude in J_s (~0.1 to 20 Am^2/kg). The region for lepidocrocite is smaller, a factor of ~25 (~0.3 to 8 Am^2/kg), but still significant. This means that Martian surface materials that are hematitic on the basis of their spectral data (e.g., the Olympus Amazonis region (Morris *et al.*, 1997)) can also have a strongly-magnetic component (maghemite) on the basis of their spectral data. We next address the issue of whether these spectrally-hematitic composites of hematite and maghemite are sufficiently magnetic to satisfy the constraints of the Viking magnetic properties experiment.

Fig. 8 is a plot of J_s versus the percentage of maghemite in our hematite-maghemite assemblages. The amount of maghemite was calculated from the magnetic data assuming value of J_s for single-phase maghemite from lepidocrocite is 50 Am^2/kg (Table 1). The two horizontal lines define the range of J_s (1-7 Am^2/kg) inferred for the Martian surface from the results of the Viking magnetic properties experiment (Hargraves *et al.*, 1979; Posey-Dowty *et al.*, 1986). The vertical dashed line at Mh/(Mh+Hm) = 60% represents the division between spectrally-hematite (lower values) and spectrally-maghemite (higher values)

samples. The diagonal line labeled "Mh+Hm=100%" corresponds to our results for pure hematite-maghemite assemblages derived from the thermal decomposition of lepidocrocite. Because values of J_s above this line are not physically possible, the stippled region in Fig. 8 represents the range of possible values of J_s and Mh/(Mh+Hm) that satisfy both spectral and magnetic constraints. Because the values of J_s for Martian surface materials are inferred from the nature of material adhering to magnets, and because the Martian regolith contains only ~18% iron as Fe_2O_3 (Clark *et al.*, 1982), the 100% line corresponds only to the physical situation where Mh-Hm assemblages have formed distinct particles (from chemical weathering) within Martian soil and were collected by the magnets. If this is the case, then Mh-Hm particles having ~2 to 12% Mh satisfy magnetic and spectral constraints. Note that this model does not require that all the iron in Martian soil be present as Mh and Hm. It only requires that some of it forms, by some mechanism, discrete particles of Mh and Hm in the stated mineralogical range.

Using various lines of evidence, Hargraves and coworkers (e.g., Hargraves *et al.*, 1979) argued that the magnetic phase in Martian soil was not present as discrete magnetic particles but was present as a component of composite particles that also included one or more weakly magnetic or nonmagnetic phases. The other diagonal lines in Fig. 8 were calculated assuming composite particles with the labeled amount of total Mh+Hm and the balance non-magnetic materials. The total amount of Mh+Hm is also the minimum chemical concentration of Fe_2O_3 in the particles. Note that as the amount of Mh+Hm decreases in the composite particles, Mh/(Mh+Hm) must increase in order for the composite particles to stay sufficiently magnetic to satisfy the Viking magnetic constraints. For example, the 36% line could correspond to the physical situation where half of the mass of the regolith is composite particles that each have 36% Fe_2O_3 as Mh-Hm assemblages (with 5%<Mh/(Mh+Hm)<40%) and the other half contains no iron and is nonmagnetic. The 18.0% line is the special case where Mh+Hm equals the total Fe_2O_3 concentration. A possible physical situation is every regolith particle has 18% Fe_2O_3 as Mh+Hm assemblages (with 10%<Mh/(Mh+Hm)<60%). Similarly, the 9.0% line could correspond to the physical situation where all regolith particles contain iron 9% Fe_2O_3 as Mh-Hm assemblages (with 22%<Mh/(Mh+Hm)<60%); the rest

of the iron (9%) is in nonmagnetic phases with no constraints on its distribution among regolith particles. The 4.5% line corresponds to the case where the range of values of Mh/(Mh+Hm) that can satisfy magnetic and spectral constraints is small (43%<Mh/(Mh+Hm)<60%), but the amount of iron that can be in other, nonmagnetic phases (13.5%) is near its maximum. The lower limit for composite particles that can satisfy the spectral and Viking magnetic constraints is 3% Mh+Hm with Mh/(Mh+Hm)=60%.

In the above discussion, the physical situation described for each value of Mh+Hm corresponds to each regolith particle having exactly the same amount of Mh+Hm. While these endmember cases are possible, they do not seem likely for complex natural samples like the Martian regolith. However, countless other situations are allowed by the stippled region in Fig. 8. For example, every particle in regoliths having composite particles with 18%<Mh+Hm<3% and can satisfy the spectral and Viking magnetic properties constraints if their values of Mh/(Mh+Hm) fall within the stippled region in Fig. 8. Composite particles having Mh+Hm>18% are also permitted in such regoliths as long as the additional chemical constraint of 18% total iron (as Fe_2O_3) is satisfied.

The magnetic properties experiment on Mars Pathfinder, which landed on the planet on July 4, 1997, was designed to better define the magnetic properties of Martian surface materials. The Pathfinder magnet array (MA) has five magnets instead of the two that were on Viking; two are essentially equivalent to the Viking magnets, and three are weaker (Smith *et al.*, 1997). Material is brought to the two Pathfinder MAs as airborne dust. In Fig. 9, which is equivalent to Fig. 8 without the Viking results, we indicate values of J, from Smith *et al.* (1997) where there is a change in the number of magnets to which material will adhere. These divisions are based on calculations assuming 1-μm diameter particles and a wind speed of 3 m/s. The number of magnets that material should adhere to is noted schematically in Fig. 9. The magnets decrease in attractive force from right to left. Note that there is no Mh+Hm composition that will adhere to all five magnets and be spectrally hematitic. The diagonal lines in Fig. 9 refer to composite particles having the indicated percentages of Mh+Hm, and the figure can be used, together with Pathfiner results, to constrain models for mineralogy of iron-bearing phases in Martian airborne dust. For example,

the material adhering to the three strongest magnets could be interpreted as particles having 36% Mh+Hm with 10%<Mh/(Mh+Hm)<40%. Because the Martian regolith has ~18% Fe_2O_3 (chemical composition, Clark *et al.*, 1982), mass-balance considerations would require that there are also soil particles with less than 18% Fe_2O_3. Models like this one are critically dependent on the values of J_s that divide the regions where material adheres to different numbers of magnets.

We tested the criteria of Smith *et al.* (1997) for magnet coverage using a copy of the Pathfinder MA (see Samples and Methods) and four of our spectrally-hematitic samples whose values of J_s range between 0.1 and 20.6 Am^2/kg. The results are shown in Fig. 10. The observation from comparing Figs. 9 and 10 is that material is adhering to more magnets than expected on the basis of the boundary J_s reported in Smith *et al.* (1997). Samples LPS2-3-500 and LPS2-3-453 (J_s = 0.1 and 0.2 Am^2/kg) should adhere to none of the magnets, but actually adhere to one and two magnets, respectively. Similarly, LPS2-3-384 and LPS2-3-352 (J_s = 3.7 and 20.6 Am^2/kg) are predicted to adhere to two and four magnets, respectively, but actually adhere to four and five magnets, respectively. At this point, we are not able to reconcile these differences. A potential explanation is differences in wind velocity, which was essentially zero (still air) in our laboratory simulations and 3 m/s in the calculations of Smith *et al.* (1997). Higher wind velocities would tend to remove material, producing observed difference between calculated and observed results. In any event, our results show that it is possible to have material that is spectrally hematitic adhering to all five magnets in the Pathfinder MA.

In summary, our results show that spectrally-hematitic composite particles of Mh+Hm produced as thermal transformation products of lepidocrocite can be sufficiently magnetic (up to ~30 Am^2/kg) to satisfy the results of the Viking magnetic properties experiment and spectral constraints for hematite. Because such material can adhere to all five Pathfinder magnets, constraints on the amount and mineralogical composition of magnetic phases within composite (multiphase) Martian dust particles can be developed from the number of magnets airborne dust actually adheres to on Mars. We conclude, therefore, that formation of lepidocrocite on Mars, perhaps by the mechanisms suggested by Posey-Dowty *et al.* (1986)

and Banin *et al.* (1993), and subsequent transformation to maghemite and hematite, perhaps by the thermal energy provided by repetitive meteoritic impact, is a way to produce spectrally-hematitic, magnetic soil on the surface of Mars. However, our spectral results are likely independent of formation mechanisms for the Mh-Hm assemblages. Thus, thermal oxidation of magnetite (Fe_3O_4) is another potential pathway to produce suitable Mh-Hm assemblages. Because magnetite is strongly magnetic, residual, unoxidixed magnetite could also contribute to the magnetic nature of Martian soil.

REFERENCES

BANIN A., BEN-SHLOMO T., MARGULIES L., BLAKE D. F., MANCINELLI R. L. AND GEHRING A. U. (1993) The nanophase iron mineral(s) in Mars soil. *J. Geophys. Res.* **98**, 20831-20853.

CLARK B. C., BAIRD A. K., WELDON R. J., TSUSAKI D. M., SCHNABEL L. AND CANDELARIA M. P. (1982) Chemical composition of martian fines. *J. Geophys. Res.* **87**, 10059-10067.

CORNELL R. AND SCHWERTMANN U. (1996) *The Iron Oxides: Structure, Properties, Reactions, Occurrences, and Uses.* VHC, New York. 573 pp.

DE BAKKER P. M. A., DE GRAVE E., VANDENBERGHE R. E., BOWEN L. H., POLLARD R. J. AND PERSOONS R. M. (1991) Mossbauer study of the thermal decomposition of lepidocrocite and characterization of the decomposition products. *Phys. Chem. Minerals* **18**, 131-143.

GEHRING A. U. AND HOFMEISTER A. M. (1994) The transformation of lepidocrocite during heating: A magnetic and spectroscopic study. *Clays Clay Minerals* **42**, 409-415.

HARGRAVES R. B., COLLINSON D. W., ARVIDSON R. V. AND SPITZER C. R. (1977) The Viking magnetic properties experiment: Primary mission results. *J. Geophys. Res.* **82**, 4547-4558.

HARGRAVES R. B., COLLINSON D. W., ARVIDSON R. E. AND CATES P. M. (1979) Viking magnetic properties experiment: Extended mission results. *J. Geophys. Res.* **84**, 8379-8384.

MORRIS R. V., GOLDEN D. C. AND BELL III J. F. (1997) Low-temperature reflectivity spectra of red

hematite and the color of Mars. *J. Geophys. Res.* **102**, 9125-9133.

MORRIS R. V. AND LAUER JR. H. V. (1981) Stability of goethite (α-FeOOH) and lepidocrocite (γ-FeOOH) to dehydration by UV radiation: Implications for their occurrence on the martian surface. *J. Geophys. Res.* 86, 10893-10899.

MORRIS R. V., LAUER JR. H. V., LAWSON C. A., GIBSON JR. E. K., NACE G. A. AND STEWART C. (1985) Spectral and other physicochemical properties of submicron powders of hematite (α-Fe_2O_3), maghemite (γ-Fe_2O_3), magnetite (Fe_3O_4), goethite (α-FeOOH), and lepidocrocite (γ-FeOOH). *J. Geophys. Res.* **90**, 3126-3144.

MORRIS R. V. AND GOLDEN D. C. (1997) Goldenrod pigments and the occurrence of hmeatite and possibly goethite in the Olympus-Anazonis region of Mars. *Icarus*, submitted.

MOSKOWITZ B. M. AND HARGRAVES R. B. (1982) Magnetic changes accompanying the thermal decomposition of nontronite (in air) and its relevance to martian mineralogy. *J. Geophys. Res.* **87**, 10,115-10,128.

MURCHIE S., MUSTARD J., BISHOP J., HEAD J., AND PIETERS C. (1993) Spatial variations in the spectral properties of bright regions on Mars. *Icarus* **105**, 454-468.

MUSTARD J. F. AND BELL III J. (1994) New composite reflectance spectra of Mars from 0.4 to 3.14 μm. *Geophys. Res. Lett.* **21**, 353-356.

POSEY-DOWTY J., MOSKOWITZ B., CRERAR D., HARGRAVES R., TANENBAUM L. AND DOWTY E. (1986) Iron oxide and hydroxide precipitation from ferrous solutions and its relevance to martian surface mineralogy. *Icarus* **66**, 105-116.

SMITH P. H., TOMASKO M. G., BRITT D., CROWE D. G., REID R. K. H. U., THOMAS N., GLIEM F., RUEFFER P., SULLIVAN R., GREELEY R., KNUDSEN J. M., MADSEN M. B., GUNNLAUGSSON H. P., HVIID S. F., GOETZ W., SOLDERBLOM L. A., GADDIS L. AND KIRK R. (1997) The imager for Mars Pathfinder experiment. *J. Geophys. Res.* **102**, 4003-4025.

TABLE 1. Magnetic (saturation magnetization J_s and mass specific susceptibility X_m) and spectral (positions of M1 maximum and T1 minimum) properties and XRD phases for samples of lepidocrocite LPS2 heated in air for various temperatures and times.

Sample	Time (hr)	Temp. (°C)	X_m ($\mu m^3/kg$)	J_s (Am^2/kg)	M1 (nm)	T1 (nm)	XRD Phases*
LPS2		20			806	962	Lp
LPS2-3-055	3.0	55	1.1	0.3	812	964	Lp
LPS2-3-110	3.0	110	1.1	0.3	807	962	Lp
LPS2-3-150	3.0	150	1.1	0.3	811	962	Lp
LPS2-3-200	3.0	200	18.5	3.3	808	966	Lp
LPS2-3-223	4.5	223	37.5	34.1	789	936	Mh+Lp
LPS2-3-233	3.0	233	37.8	42.9	787	928	Mh+Lp
LPS2-3-265	3.0	265	40.2	48.0	778	886	Mh>>Hm
LPS2-3-323	3.0	323	21.0	29.5	752	863	Mh+Hm
LPS2-3-352	2.8	352	13.1	20.6	745	861	Mh+Hm
LPS2-3-384	2.8	384	2.6	3.7	740	860	Hm>>Mh
LPS2-3-453	3.0	453	0.2	0.2	740	861	Hm
LPS2-3-500	3.0	500	0.0	0.1	739	861	Hm
LPS2-300-145	305	145	1.2	0.4	807	965	Lp
LPS2-300-163	329	163	21.7	5.3	795	757	Lp>>Hm+Mh
LPS2-300-170	307	170	26.9	6.4	797	954	Lp>>Hm+Mh
LPS2-300-197	305	197	38.6	49.8	775	898	Mh>>Hm
LPS2-300-223	296	223	37.6	49.4	772	905	Mh>>Hm
LPS2-300-252	285	252	25.4	41.8	755	870	Mh+Hm
LPS2-300-525	333	525	0.0	0.1	740	862	Hm
uncertainty		±5	±10%	±0.1	±6	±6	

* Lp = lepidocrocite (γ-FeOOH); Mh = maghemite (γ-Fe_2O_3); Hm = hematite (α-Fe_2O_3).

Figure Captions

Fig. 1. XRD spectra for LPS2 and products obtained from it by heating at various temperatures for 3 hr. Heating temperatures and saturation magnetizations are indicated down the left and right sides, respectively. Indexes of diffraction lines unique to lepidocrocite (orthorhombic [020], [120], [051], and [200]) , maghemite (tetragonal [220] and [440]), and hematite (hexagonal [012], [104], and [113]) are indicated.

Fig. 2. Comparison of XRD data for LPS2-3-265 and LPS2-300-223, the most Mh-rich samples we obtained from dehydroxylation of lepidocrocite, and MHS3, a maghemite commercially prepared by reduction of goethite to magnetite followed by oxidation magnetite to maghemite. The narrow lines and presence of Mh superlattice lines for MHS3 result from the vacancy ordering and good crystallinity that is not present in the other two maghemites.

Fig. 3. Electron micrographs and electron diffraction (ED) patterns (insets) of dispersed particles: (a) Unheated lepidocrocite (LPS2); ED spots correspond to lepidocrocite spacings, and each particle is a single crystal. (b) LPS2-3-223; ED pattern consisting of diffuse streaky spots corresponding to lepidocrocite and maghemite. (c) LPS2-3-265; ED pattern corresponds entirely to that of maghemite, and each particle is polycrystalline maghemite. (d) LPS2-3-323; ED pattern corresponds to hematite and maghemite. (e) LPS2-3-500; ED pattern corresponds entirely to that of hematite, and each particles is polycrystalline hematite. (f) Magnified image of (e) showing the curved lath-ends. The two diffuse rings in most patterns result from the carbon substrate.

Fig. 4. Magnetic properties of transformation products of LPS2: (a) J_s and (b) X_m, both at 20°C. Closed squares denote ~300 hr heating periods, and open circles denote ~3 hr heating periods. The bell-shaped curve results from the strongly magnetic nature of maghemite compared to lepidocrocite and hematite.

Fig. 5. Diffuse reflectivity spectra (20°C) LPS2 and samples obtained from it by heating at various temperatures for ~3 hr. The spectra are grouped according to whether they are most like lepidocrocite, maghemite, or hematite. M1 and T1 are the lowest-energy maximum and minimum, respectively, that can be associated with ferric spectral features.

Fig. 6. Plot of the positions of the M1 and T1 spectral features (20°C) as a function of heating temperature for both 3 hr and 300 hr heating periods. The positions of the spectral features for maghemite are intermediate to those for lepidocrocite and hematite.

Fig. 7. Plot of J_s as a function of positions of M1 and T1 spectral features (20°C). Note that Mh+Hm assemblages made from lepidocrocite can have values of J_s up to ~20 Am^2/kg and, spectrally speaking, be hematite.

Fig. 8. Plot of J_s (20°C) versus Mh/(Mh+Hm) for Viking results. The stippled region represents values of J_s and Mh/(Mh+Hm) that satisfy the constraints of the Viking magnetic properties experiment and Martian spectral data. The solid diagonal lines represent various concentrations (in wt. %) of Mh+Hm in hypothetical samples. Chemically, Martian soil has ~18% Fe_2O_3 (Clark *et al.*, 1982).

Fig. 9. Plot of J_s (20°C) versus Mh/(Mh+Hm) for the Pathfinder magnetic properties experiment. The stippled region represents values of J_s and Mh/(Mh+Hm) that are physically allowed and are spectrally hematitic. The horizontal lines are the values of J_s from Smith *et al.* (1997) which were calculated assuming 1 μm particles and a wind speed of 3 m/s.

Fig. 10. Results of MA simluations done with four spectrally-hematitic powders: (a) LPS2-3-352, attracted to all 5 magnets. (b) LPS2-3-384, attracted to 4 magnets. (c) LPS2-3-453, attracted to 2 magnets (d) LPS2-3-352, attracted to 1 magnet. The saturation magnetizations (J_s) are indicated in the figure. The magnets decrease in attractive force from right to left. The MA was made at the Oersted Laboratory, Niels Bohr Institute for Astronomy, Physics, and Geophysics, University of Copenhagen, Denmark, and provided courtesy of Drs. Jens Martin Knudsen and Morton Bo Madsen.

Fig. 1, Morris et al. (1997), Lepidocrocite to maghemite to hematite...

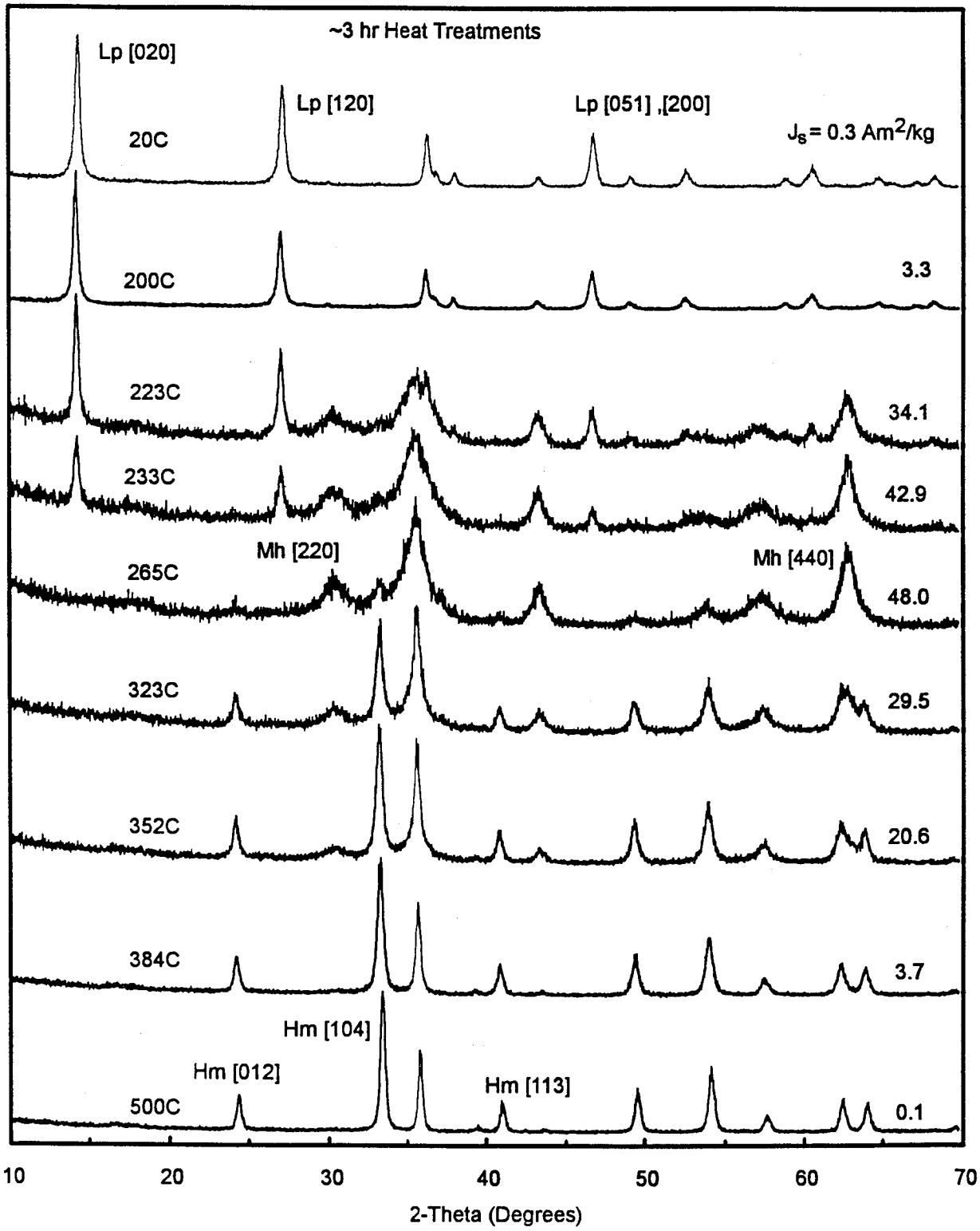

Fig. 2, Morris et al. (1997), Lepidocrocite to maghemite to hematite...

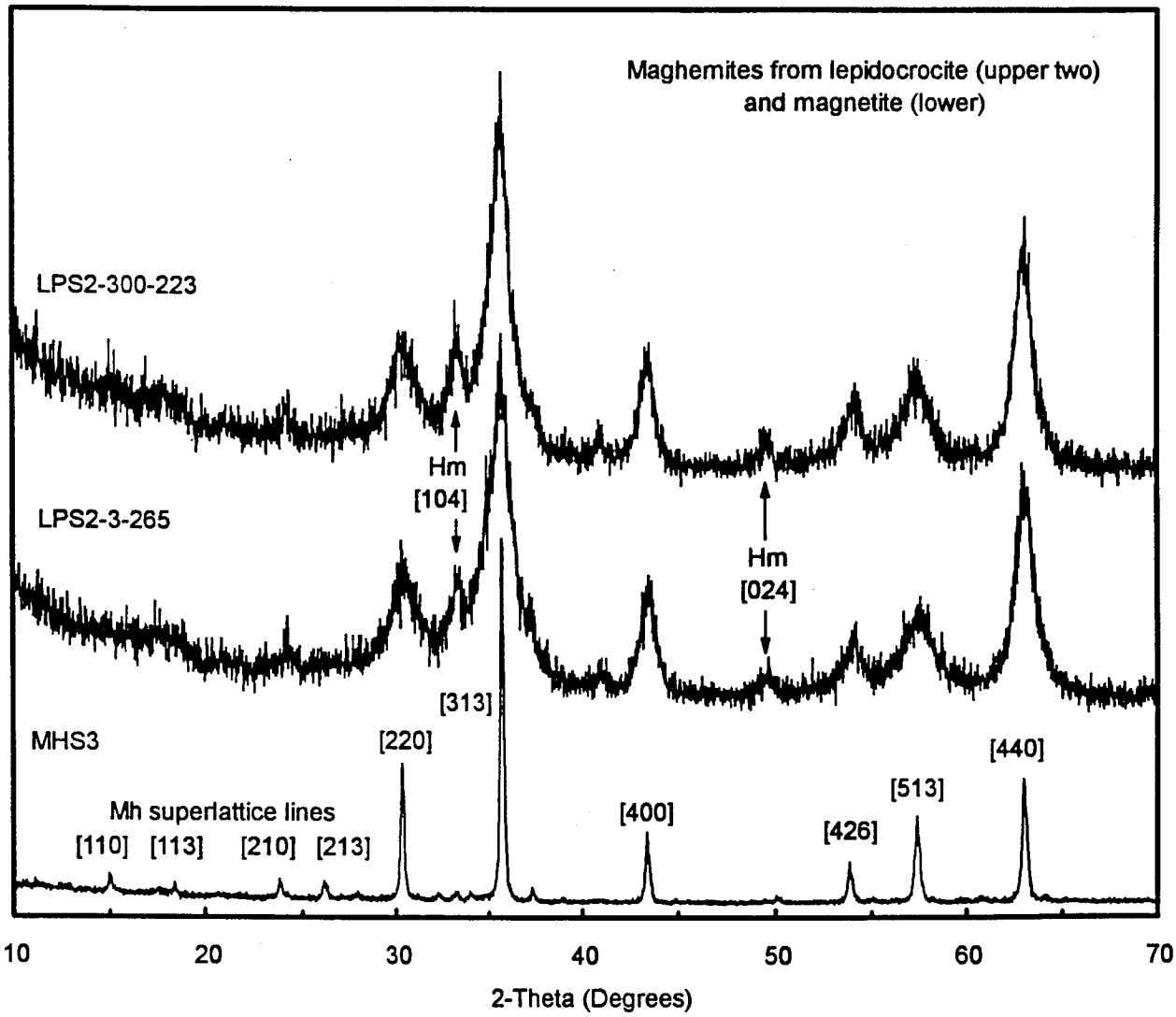

Fig. 3, Morris et al. (1997), Lepidocrocite to maghemite to hematite....

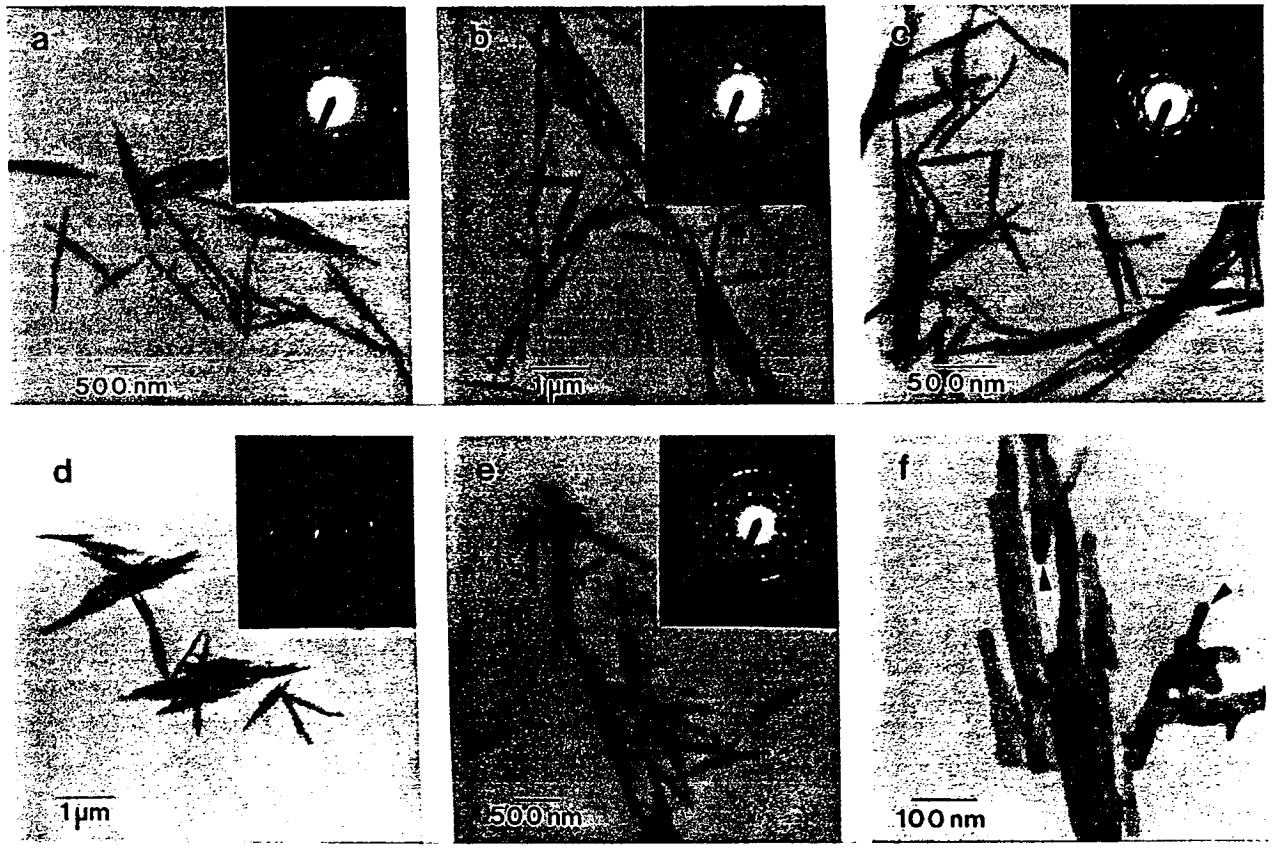

Fig. 4, Morris et al. (1997), Lepidocrocite to maghemite to hematite...

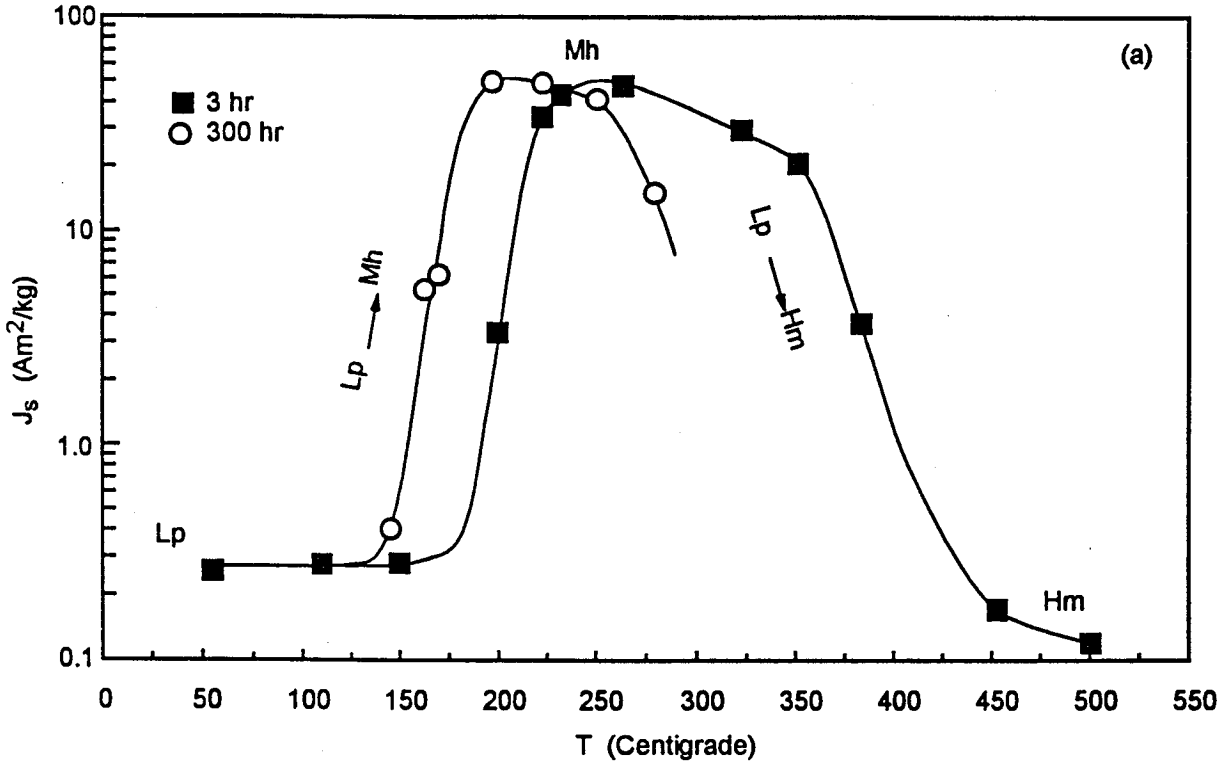

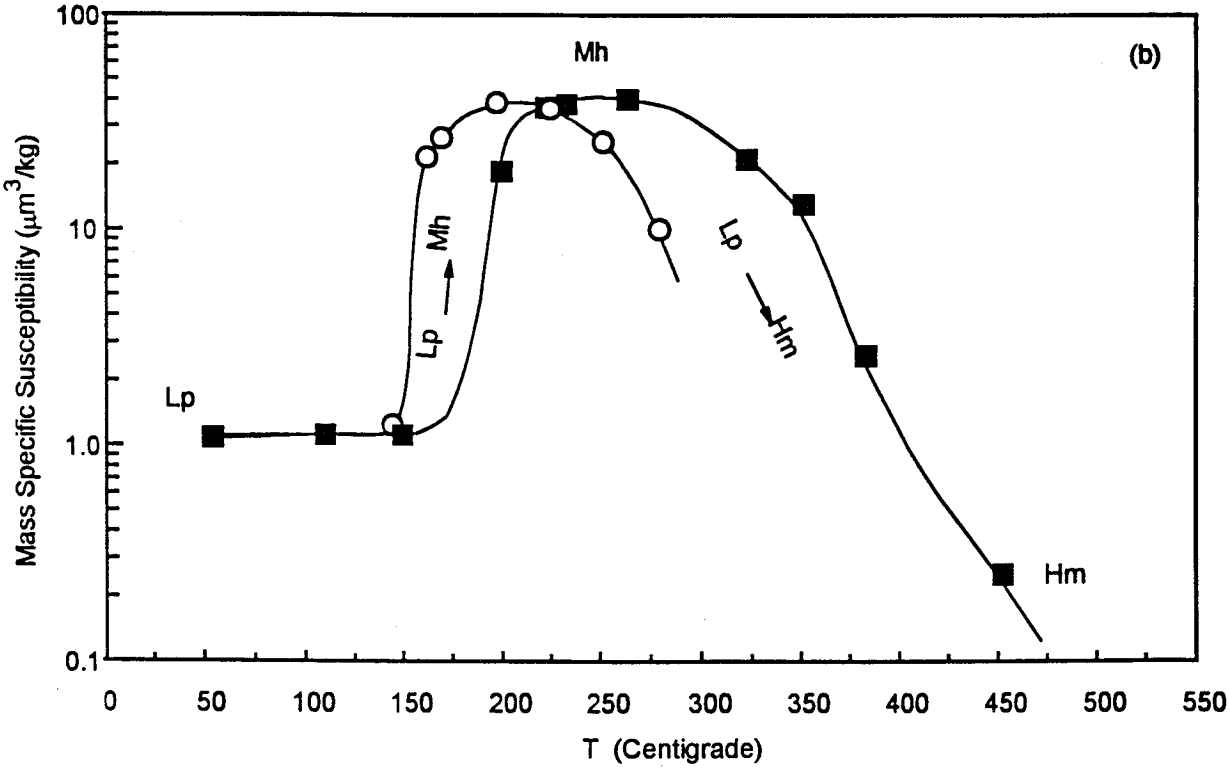

Fig. 5, Morris et al. (1997), Lepidocrocite to maghemite to hematite...

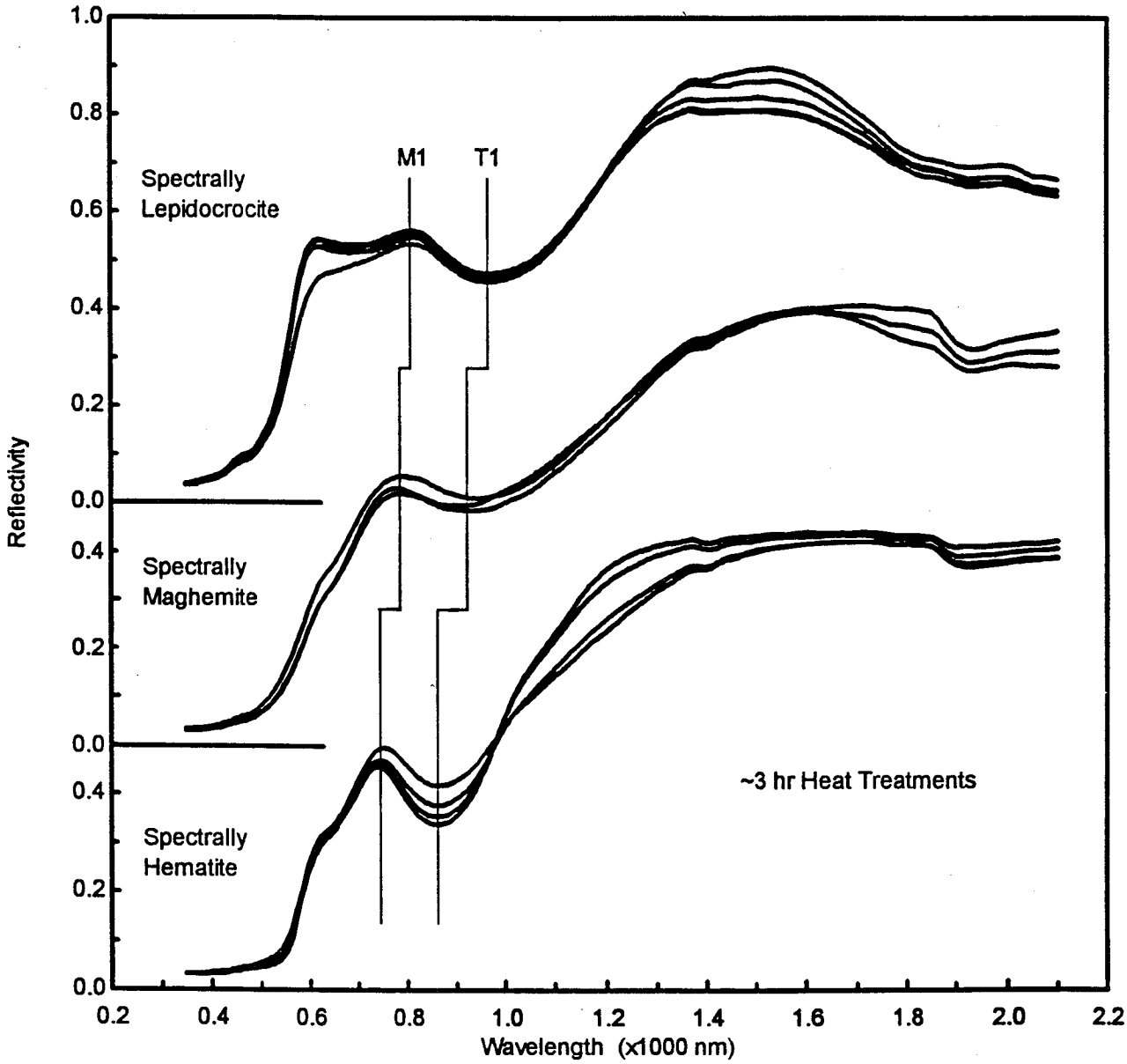

Fig. 6, Morris et al. (1997), Lepidocrocite to maghemite to hematite....

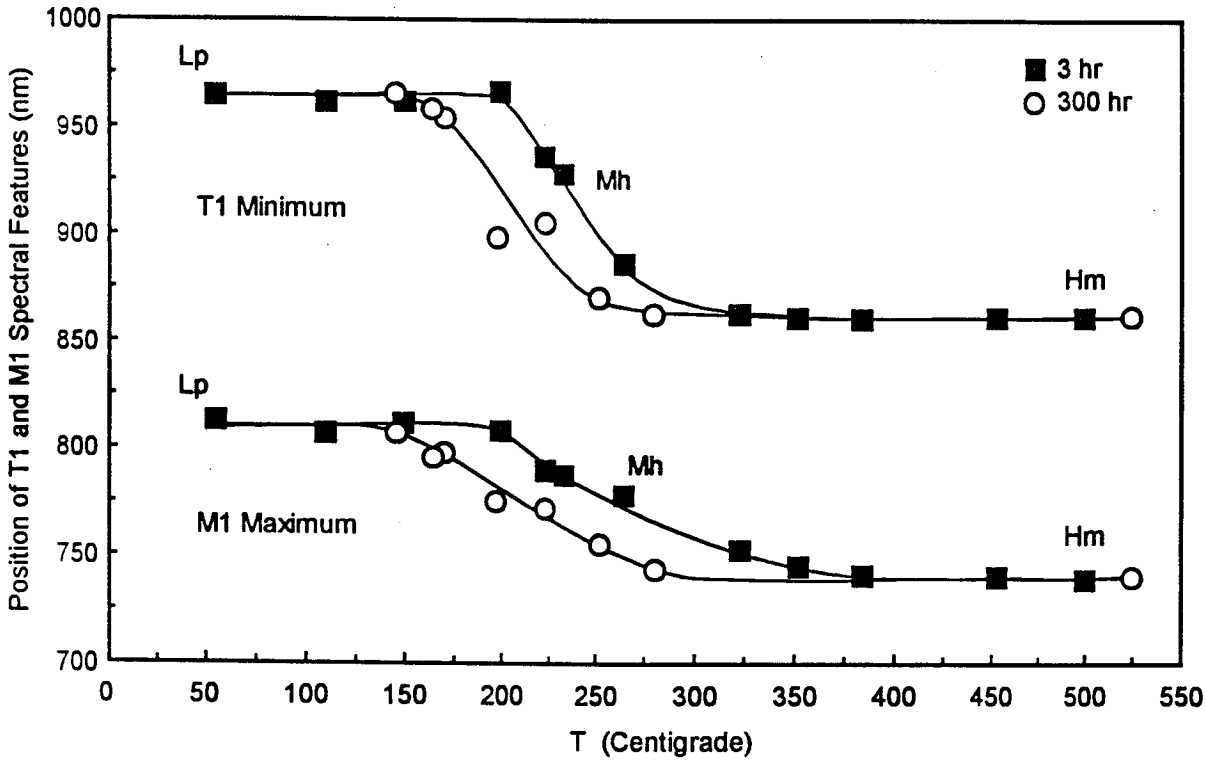

Fig. 7, Morris et al. (1997), Lepidocrocite to maghemite to hematite...

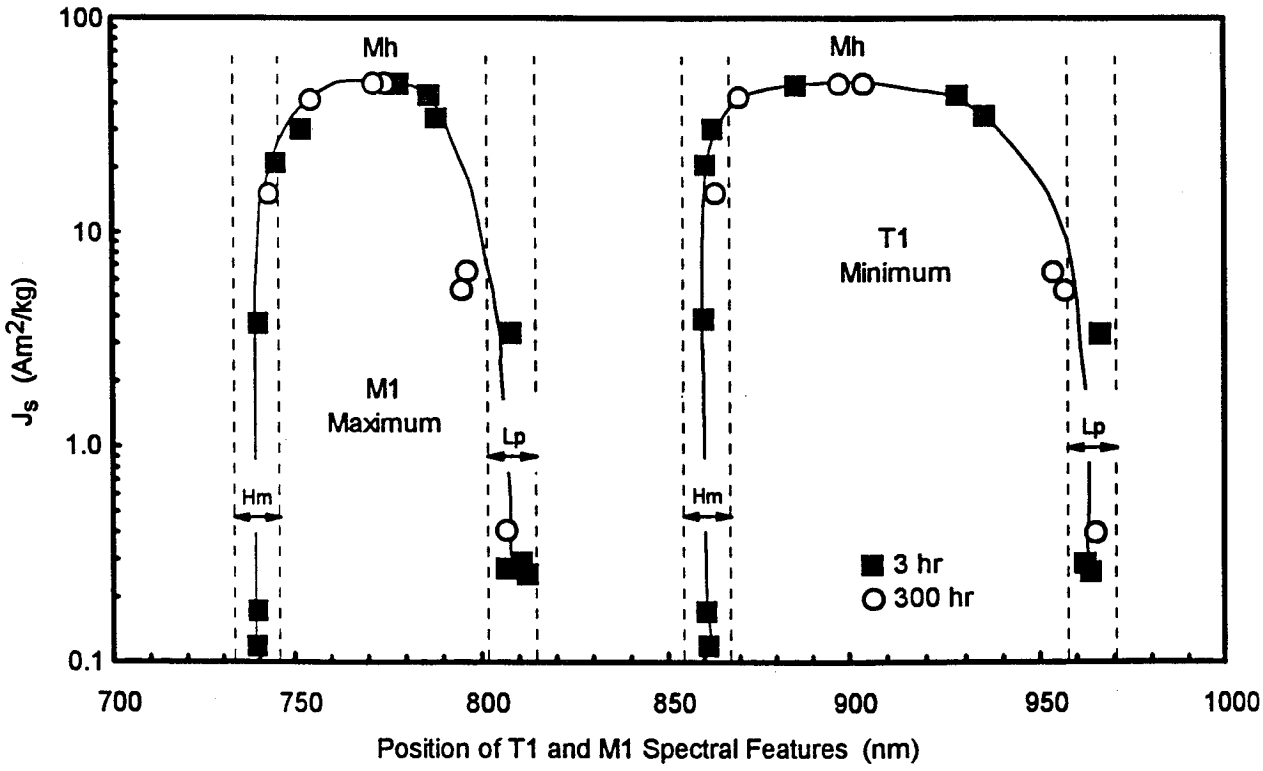

Fig. 8, Morris et al. (1997), Lepidocrocite to maghemite to hematite...

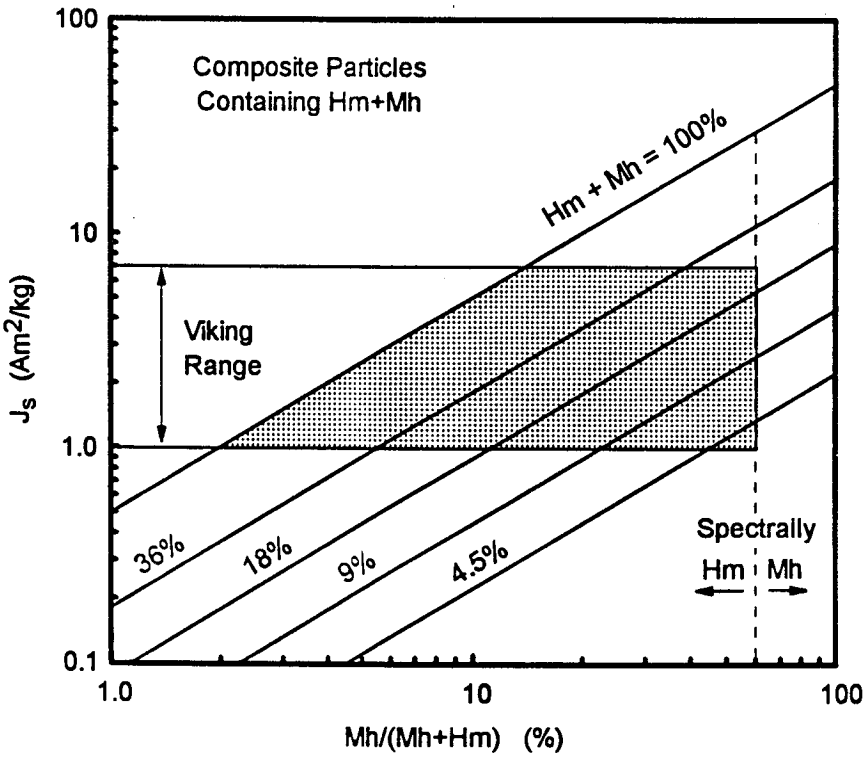

Fig. 9, Morris et al. (1997), Lepidocrocite to maghemite to hematite...

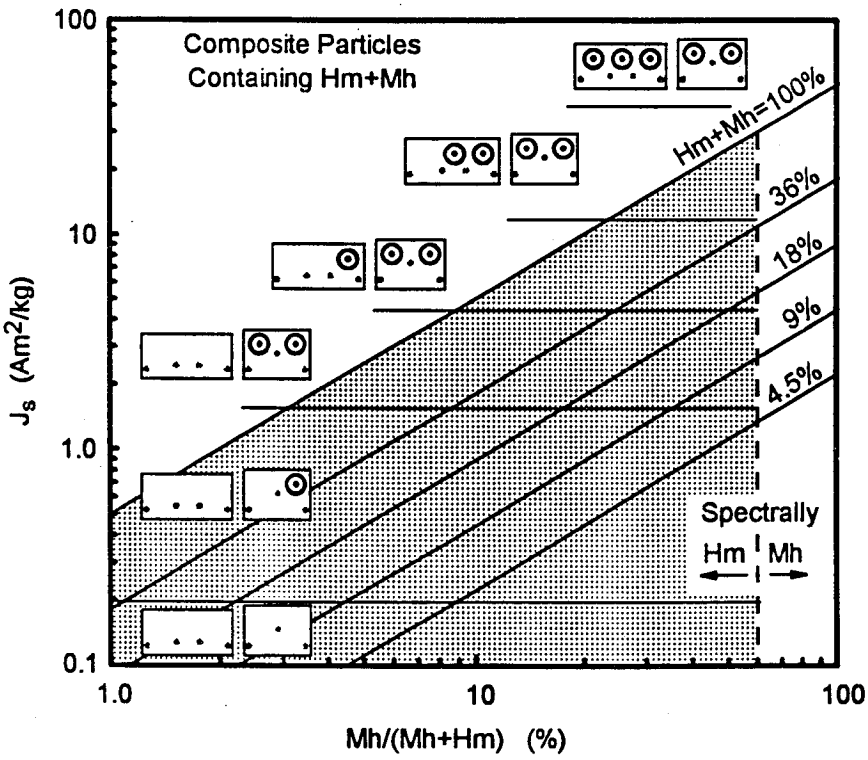

Fig. 10, Morris et al. (1997), Lepidocrocite to maghemite to hematite...